The Products of the Thermal Decomposition of CH_3CHO

AnGayle Vasiliou,[1,3] Krzysztof M. Piech,[1] Xu Zhang,[2]
Mark R. Nimlos,[3] Musahid Ahmed,[4] Amir Golan,[4] Oleg Kostko,[4] David L. Osborn,[5] John W. Daily,[6] John F. Stanton,[7] and G. Barney Ellison[1]

[1] Department of Chemistry and Biochemistry
University of Colorado
Boulder, CO 80309-0215
Email: barney@jila.colorado.edu

[2] Jet Propulsion Laboratory
California Institute of Technology
4800 Oak Grove Drive
Pasadena, CA 91109-8099
Email: xu.zhang@jpl.nasa.gov

[3] National Renewable Energy Laboratory
1617 Cole Blvd.
Golden, CO 80401
Email: mark_nimlos@nrel.gov

[4] Chemical Sciences Division
LBNL MS 6R-2100
Berkeley CA 94720
Email: mahmed@lbl.gov

[5] Combustion Research Facility
Sandia National Laboratories
PO Box 969 MS 9055
Livermore, CA 94551-0969
Email: dlosbor@sandia.gov

[6] Center for Combustion and Environmental Research
Department of Mechanical Engineering
University of Colorado at Boulder
Boulder, CO 80309-0427
Email: john.daily@colorado.edu

[7] Institute for Theoretical Chemistry
Department of Chemistry
University of Texas
Austin, TX 78712
Email: jfstanton@mail.utexas.edu

[submitted to *J. Chem. Phys.*, March 2011]

Abstract

We have used a heated 2 cm x 1 mm SiC microtubular (μtubular) reactor to decompose acetaldehyde: $CH_3CHO + \Delta \rightarrow$ products. Thermal decomposition is followed at pressures of 75 — 150 Torr and at temperatures up to 1700 K, conditions that correspond to residence times of roughly 50 — 100 μsec in the μtubular reactor. The acetaldehyde decomposition products are identified by two independent techniques: VUV photoionization mass spectroscopy (PIMS) and infrared (IR) absorption spectroscopy after isolation in a cryogenic matrix. Besides CH_3CHO, we have studied three isotopologues, CH_3CDO, CD_3CHO, and CD_3CDO. We have identified the thermal decomposition products CH_3 (PIMS), CO (IR, PIMS), H (PIMS), H_2 (PIMS), CH_2CO (IR, PIMS), CH_2=CHOH (IR, PIMS), H_2O (IR, PIMS), and HC≡CH (IR, PIMS). Plausible evidence has been found to support the idea that there are at least three different thermal decomposition pathways for CH_3CHO:

Radical decomposition: $CH_3CHO + \Delta \rightarrow CH_3 + [HCO] \rightarrow CH_3 + H + CO$

Elimination: $CH_3CHO + \Delta \rightarrow H_2 + CH_2=C=O$

Isomerization/elimination: $CH_3CHO + \Delta \rightarrow [CH_2=CH\text{-}OH] \rightarrow HC\equiv CH + H_2O$

Both PIMS and IR spectroscopy show compelling evidence for the participation of vinylidene, $CH_2=C\mathbf{:}$, as an intermediate in the decomposition of vinyl alchohol: $CH_2=CH\text{-}OH + \Delta \rightarrow [CH_2=C\mathbf{:}] + H_2O \rightarrow HC\equiv CH + H_2O$

The thermal decomposition of acetaldehyde has been extensively studied in shock tubes, flow reactors, and flames over the last 75 years.[1-12] The weakest bond in acetaldehyde[13] is the CH_3-CHO linkage. It is commonly accepted that the major thermal decomposition channel is formation of radicals *via* cleavage of the C-C bond:

$$CH_3CHO + \Delta \rightarrow CH_3 + HCO \qquad (1)$$

The formyl radical (HCO) is only weakly bound[13] and will not survive for long at temperatures over 1300 K. The dynamics of the thermal cracking of CH_3CHO are generally modeled as a sequence of radical reactions.[14,15] Recently, it has been reported that acetaldehyde could thermally decompose by a roaming process.[12] Roaming mechanisms[16-18] are characterized by formation of a dynamically-bound complex of radicals that subsequently disproportionates. The products are not radicals but closed shell species; in this case, methane and carbon monoxide: $CH_3CHO + \Delta \rightarrow [CH_3\bullet, \bullet HCO] \rightarrow CH_3$-H + CO.

We have studied the thermal cracking of CH_3CHO in a heated microtubular (μtubular) reactor,[19,20] a 1 mm i.d. x 2 cm long SiC tube that can be heated to temperatures up to 1700 K. A dilute sample of acetaldehyde is mixed with an inert carrier gas and passed through the heated SiC tube. Gases exiting the μtubular reactor emerge in an under-expanded jet at roughly 10^{-5} Torr. The translational, vibrational, and rotational temperatures drop rapidly within a few diameters and all chemistry ceases. The products are identified by their photoionization (PIMS) mass spectra as well as their matrix infrared absorption spectra. The PIMS experiment uses a reflectron time-of-flight mass spectrometer to analyze the ions resulting from photoionization by 118.2 nm (10.487 eV) photons.[19] In separate experiments, we send a gas mixture of CH_3CHO in Ar

carrier gas through the μtubular reactor and the resultant molecular beam impinges on a CsI window cooled to 20 K. The matrix frozen onto the CsI window is subsequently analyzed by IR absorption spectroscopy.[21] Additional experiments were carried out at the chemical dynamics beamline (9.0.2) at the LBNL Advanced Light Source (ALS),[22,23] where PIMS spectra can be obtained as a function of photon energy, which also allows for the recording of photoionization efficiency (PIE) profiles.

The dynamics of pyrolysis and transport through the SiC μtubular reactor is poorly characterized. Preliminary computational fluid dynamics[24] simulations estimate that the gas pressure in the μtubular reactor is about 10% of the stagnation pressure. Within the reactor, there is a range of temperatures within the gas as it is heated by the walls. As a result, not all molecules see the same temperature time history. In reactor language there is a residence time distribution. However, as the gas approaches the tube exit, it is fairly uniformly heated such that the centerline temperature is within 100 – 200 K of the wall temperature. From simulations[24] of the gas velocity, we estimate the residence time within the heated SiC tube to be roughly 50 — 100 μsec.

When acetaldehyde and its isotopologues are thermally decomposed in the μtubular reactor, the products monitored by 118.2 nm (10.487 eV) PIMS are shown in Fig. 1. The bottom trace in Fig. 1 shows the products resulting from heating CH_3CHO to 1500 K. We observe the CH_3CHO^+ cation at m/z 44 as well as a feature at m/z 43. The latter is tentatively[25] attributed to the acetyl cation, CH_3CO^+, *via* dissociative ionization of vibrationally excited acetaldehyde, a process for which the room temperature threshold has been established to be approximately 10.8 eV. We also observe the ketene cation, CH_2CO^+, at m/z 42, and CH_3^+ at m/z 15. The second trace in Fig. 1 is that of CH_3CDO. The species at m/z 45 is the parent peak of CH_3CDO^+ and a dissociative

ionization product, analogous to the m/z 43 peak found for CH_3CHO, is observed. The cation of ketene is found at m/z 42. As expected, we observe the CH_3^+ ion at m/z 15. Surprisingly we also detect the CDH_2^+ and CD_2H^+ ions at m/z 16 and 17. The third trace in Fig. 1 is that of CD_3CHO heated to 1500 K. The bands at m/z 47 and 46 are the parent and the product of the aforementioned dissociative ionization process. The feature at m/z 44 is that of $CD_2{=}C{=}O^+$. The perdeuterated methyl cation is observed at m/z 18 and we also observe signals from CD_2H^+(17), CDH_2^+(16), and CH_3^+ (15). Examination of the PIE curves[26] demonstrates that the signals in Fig. 1 at m/z 15, 16, 17, and 18 all result from ionization of methyl radicals.[27] The final spectrum in Fig. 1 is that of CD_3CDO heated to 1500 K. Peaks for the parent cation, m/z 48, and that for dissociative ionization, m/z 46, are detected. The weak band at m/z 47 is assigned as CHD_2CDO^+ and arises from a known contamination (roughly 2%) of the CD_3CDO sample.[28] The band at m/z 44 is that of $CD_2{=}C{=}O^+$ while that at m/z 18 is CD_3^+.

A portion of the matrix IR absorption spectra resulting from the thermal cracking of acetaldehyde[29] is shown in Fig. 2. The bottom trace (green) is a control scan of the Ar carrier gas after passing through the μtubular reactor heated to 1700 K. The black scan is that of CH_3CHO/Ar exposed to the same conditions. The peak at 3619 cm^{-1} is assigned[30-32] to the O-H stretch of vinyl alcohol, $\nu_1(CH_2CHO\text{-}H)$, while the bands at 3302 cm^{-1} and 3288 cm^{-1} belong to acetylene, $\nu_3(HCCH)$, and are the absorptions associated with the well-known Darling-Dennison mixing of ν_3 and $\nu_2 + \nu_4 + \nu_5$. The red trace in Fig. 2 is that for CH_3CDO at the same conditions. The peak at 3621 cm^{-1} is that[31] of $\nu_1(CH_2CDO\text{-}H)$ and the features of HCCH at 3302 cm^{-1} and 3288 cm^{-1} are present. In addition to these features, the red trace in Fig. 2 clearly shows the C-H and C-D bands belonging to acetylene-d_1, HCCD, at 3323 cm^{-1} (ν_1) and 2587 cm^{-1} (ν_3), which has

significant mechanistic implications, as discussed below.

Matrix IR spectroscopy[26] from the products of heated CH_3CHO or CH_3CDO also shows bands[33] belonging to CO and CH_2=C=O. When CD_3CHO or CD_3CDO are thermally cracked at 1700 K, the characteristic O-D stretches of the corresponding vinyl alcohols, $\nu_1(CD_2CHO\text{-}D)$ at 2674 cm^{-1} and $\nu_1(CD_2CDO\text{-}D)$ = 2675 cm^{-1}, are detected. When either CD_3CHO or CD_3CDO is pyrolyzed, IR signals from CD_2=C=O, D_2O, and HOD are observed. Equations (2) — (5) summarize the results of the matrix IR spectra:

$$CH_3CHO + 1400^o \rightarrow CO \oplus CH_2CO \oplus CH_2{=}CHOH \oplus H_2O \oplus HC{\equiv}CH \quad (2)$$

$$CH_3CDO + 1400^o \rightarrow CO \oplus CH_2CO \oplus CH_2{=}CDOH \oplus [H_2O \oplus HC{\equiv}CD] \text{ and } [HOD \oplus HC{\equiv}CH] \quad (3)$$

$$CD_3CHO + 1400^o \rightarrow CO \oplus CD_2CO + CD_2{=}CHOD \oplus [D_2O \oplus DC{\equiv}CH] \text{ and } [HOD \oplus DC{\equiv}CD] \quad (4)$$

$$CD_3CDO + 1400^o \rightarrow CO \oplus CD_2CO \oplus CD_2{=}CDOD \oplus D_2O \oplus DC{\equiv}CD \quad (5)$$

Fig. 3 shows the PIMS resulting from cracking CD_3CHO at 1200° when the ALS synchrotron is used to photoionize the pyrolysis products. In Fig. 3, $\hbar\omega_{VUV}$ is set to 12.9 eV, which is sufficient to ionize acetylene, methane, and water.[27] The features at m/z 19 and 20 are identified[34] by the associated PIE curves as HOD^+ and D_2O^+ as are the peaks at m/z 26, 27, and 28 to $HCCH^+$, $DCCH^+$, and $DCCD^+$. The tiny $HCCH^+$ signal is an artifact arising from the aforementioned impurity in the CD_3CHO sample.[28]

One might be concerned that some of the acetaldehyde chemistry could be resulting from wall reactions. The PIMS spectra in Fig. 1 demonstrate that methyl radicals are exchanging H atoms. Thermal decomposition of CH_3CDO in Fig. 1 will generate both CH_3 and D atoms. If there are rapid homogeneous, radical/radical

reactions in the μtubular reactor, chemically activated methane will be produced. The product methane will be activated by the CH_3-D bond energy[13] and CH_3D^* would not be expected to survive in the hot SiC tube: $CH_3 + D \rightleftharpoons CH_3D^* \rightleftharpoons CH_2D + H$. This interpretation is one explanation for the H atom exchanges of both CH_3CDO and CD_3CHO in Fig. 1. If methyl radicals are abstracting H atoms from the walls of the SiC tube, we would expect to find that the CD_3 radicals from CD_3CDO decomposition would be scrambled by ^{1}H-dominated wall chemistry: $CD_3 \rightarrow [CHD_2, CDH_2, CH_3]$. However the CD_3 radicals produced by cracking CD_3CDO do not undergo H/D exchange; only signals at m/z 18 are observed, implying that hydrogen exchange chemistry on the reactor walls is negligible.

Besides H atom abstractions from the wall, one might also be concerned about proton-catalyzed reactions at the wall. The IR spectra clearly detect the presence of vinyl alcohol when CH_3CHO is cracked. The classical mechanism[35] for keto-enol tautomerization is by proton catalysis. Consequently H^+ catalysis by the SiC walls would predict that CD_3CHO would isomerize to CD_2=CH-OH. This is not observed; the matrix IR following 1500 K decomposition of CD_3CHO clearly detects the O-D stretch of the product vinyl alcohol, $\nu_1(CD_2CHO\text{-}D)$; the corresponding spectral feature from CD_2CHO-H is not observed. The ALS PIMS results confirm this conclusion.

It is natural to wonder how the present results might relate to the proposed roaming pathway[12] for acetaldehyde decomposition. Any methane formed by roaming would be chemically activated by roughly 4 eV and is unlikely to survive in the hot μtubular reactor. Hence, the fact that we do not observe prominent spectral signatures of methane in this work – indeed, no trace of methane is seen in the IR studies[36] – is not particularly illuminating; it does not suggest that methane is not formed *via* roaming

under the reaction conditions. What does seem clear is that the additional pathways for acetaldehyde decomposition observed here should be included in models of this important reaction.

Table 1 is a summary of our experimental findings. It is certain that the decomposition of CH_3CHO in the μtubular reactor is a significantly more complicated process than that implied by the simple picture provided by (1). Our results are consistent with three different decomposition channels.

$$CH_3CHO + \Delta \rightarrow CH_3 + [HCO] \rightarrow CH_3 + H + CO \qquad \text{radical decomposition (6)}$$

$$CH_3CHO + \Delta \rightarrow H_2 + CH_2{=}C{=}O \qquad \text{elimination (7)}$$

$$CH_3CHO + \Delta \rightarrow [CH_2{=}CH\text{-}OH] \rightarrow HC{\equiv}CH + H_2O \qquad \text{isomerization/elimination (8)}$$

The detection of HOD and D_2O from the cracking of CD_3CHO in Fig. 3 demonstrates that vinyl alcohol can decompose by a (1,2) elimination, eq. (9), as well as by a (1,1) elimination, eq. (10). The latter pathway generates the well-known but fleeting reactive intermediate, vinylidene, which rapidly rearranges to acetylene with a negligible energy barrier:

$$CD_2{=}CH\text{-}OD \rightarrow DC{\equiv}CH + D_2O \qquad (9)$$

$$CD_2{=}CH\text{-}OD \rightarrow [CD_2{=}C{:}] + HOD \rightarrow DC{\equiv}CD + HOD \qquad (10)$$

In Fig. 3 the peak intensities of HOD^+ and $DCCD^+$ are about twice that of D_2O^+ and $DCCH^+$. This ratio suggests that (1,1) elimination *via* the $CD_2{=}C{:}$ carbene is favored over direct-(1,2) elimination, although more careful quantitative work is needed to draw any definitive conclusion. The present work, however, provides evidence that the

vinylidene channel is at least competitive with the (1,2) elimination. In a related system, it is known that (1,1) elimination is 3 times more likely than (1,2) elimination in vinyl chloride photodissociation, CH_2=CHCℓ + $\hbar\omega$ → HC≡CH + HCℓ, where HCℓ loss occurs on the ground electronic state.[37]

Vinylidene is one of the most fundamental carbenes and its properties and the [CH_2=C**:** → HC≡CH] isomerization dynamics have been the subject of many investigations.[38-45] Several previous workers[46-48] had suspected the importance of vinyl alcohol in acetaldehyde decomposition. There are few predictions of the role of HC≡CH and, especially, CH_2=C**:** in the decomposition of acetaldehyde. Besides vinylidene, we also considered the possibility that the methylhydroxycarbene,[49] CH_3-C-OH, might be a participant in the thermal decomposition of CH_3CHO; however we believe that this is unlikely.[50]

Acknowldegements: : We would like to acknowledge support from the United States Department of Energy (grant: DE-FG02-93ER14364), the United States Department of Energy's Office of the Biomass Program (Contract no. 1544759) and the National Science Foundation (CHE-0848606) (grant: CHE-0848606) for JWD, JFS, MRN, and GBE. KMP was supported by the Swiss National Science Foundation. XZ would like to acknowledge support from the NASA Planetary Atmospheres Program. MA, AG, OK and the ALS are supported by the Director, Office of Energy Research, Office of Basic Energy Sciences, and Chemical Sciences Division of the U.S. Department of Energy under contracts No. DE-AC02-05CH11231. DLO is supported by the Division of Chemical Sciences, Geosciences and Biosciences, the Office of Basic Energy Sciences, the U.S. Department of Energy. Sandia is a multiprogram laboratory operated by Sandia Corporation, a Lockheed Martin Company, for the National Nuclear Security Administration under Contract No. DE-AC04-94-AL85000. JFS also acknowledges support from the Robert A. Welch Foundation (Grant F-1283) and the United States Department of Energy, Basic Energy Sciences. Finally, we would like to thank Professors John R. Barker, William H. Green, Anne B. McCoy and Robert J. McMahon for provocative discussions.

References

(1) Rice, F. O.; Herzfeld, K. F. *Journal of the American Chemical Society* **1934**, *56*, 284.

(2) Colket, M. B.; Naegeli, D. W.; Glassman, I. *International Journal of Chemical Kinetics* **1975**, *7*, 223.

(3) Ernst, J.; Spindler, K. *Berichte Der Bunsen-Gesellschaft-Physical Chemistry Chemical Physics* **1975**, *79*, 1163.

(4) Ernst, J.; Spindler, K.; Wagner, H. G. *Berichte Der Bunsen-Gesellschaft-Physical Chemistry Chemical Physics* **1976**, *80*, 645.

(5) Kaiser, E. W.; Westbrook, C. K.; Pitz, W. J. *International Journal of Chemical Kinetics* **1986**, *18*, 655.

(6) Cavanagh, J.; Cox, R. A.; Olson, G. *Combustion and Flame* **1990**, *82*, 15.

(7) Dagaut, P.; Reuillon, M.; Voisin, D.; Cathonnet, M.; McGuinness, M.; Simmie, J. M. *Combustion Science and Technology* **1995**, *107*, 301.

(8) Gupte, K. S.; Kiefer, J. H.; Tranter, R. S.; Klippenstein, S. J.; Harding, L. B. *Proceedings of the Combustion Institute* **2007**, *31*, 167.

(9) Bentz, T.; Striebel, F.; Olzmann, M. *Journal of Physical Chemistry A* **2008**, *112*, 6120.

(10) Yasunaga, K.; Kubo, S.; Hoshikawa, H.; Kamesawa, T.; Hidaka, Y. *International Journal of Chemical Kinetics* **2008**, *40*, 73.

(11) Leplat, N.; Vandooren, J. *Combustion Science and Technology* **2010**, *182*, 436.

(12) Sivaramakrishnan, R.; Michael, J. V.; Klippenstein, S. J. *Journal of Physical Chemistry A* **2010**, *114*, 755.

(13) Some Bond Dissociation Energies are: $D_0(CH_3\text{-}CHO)$ = 83.0 ± 0.2 kcal mol^{-1}; $D_0(CH_3CO\text{-}H)$ = 87.9 ± 0.4 kcal mol^{-1}; $D_0(H\text{-}CH_2CHO)$ = 95 ± 1 kcal mol^{-1}; $D_0(H\text{-}CO)$ = 14.4 ± 0.1 kcal mol^{-1}; $D_0(CH_3\text{-}H)$ = 103.4 ± 0.1 kcal mol^{-1}; $\Delta_{rxn}H_0(CH_3CHO \rightarrow CH_4 + CO)$ = -6.0 ± 0.1 kcal mol^{-1}; $\Delta_{rxn}H_0(CH_3CHO \rightarrow HCCH + H_2O)$ = 34.5 ± 0.5 kcal mol^{-1}; $\Delta_{rxn}H_0(CH_3CHO \rightarrow H_2 + CH_2{=}C{=}O)$ = 19.7 ± 0.2 kcal mol^{-1}

(14) Benson, S. W. *Foundations of Chemical Kinetics*; McGraw Hill: New York, 1960.

(15) Houston, P. L. *Chemical Kinetics and Reaction Dynamics*, Dover Ed. ed.; Dover Publications, Inc.: Mineola, New York, 2006. Example 2.7: The Rice Herzfeld Mechanism for Decomposition of Acetaldehyde, p. 74

(16) Houston, P. L.; Kable, S. H. *Proceedings of the National Academy of Sciences of the United States of America* **2006**, *103*, 16079.

(17) Heazlewood, B. R.; Jordan, M. J. T.; Kable, S. H.; Selby, T. M.; Osborn, D. L.; Shepler, B. C.; Braams, B. J.; Bowman, J. M. *Proceedings of the National Academy of Sciences of the United States of America* **2008**, *105*, 12719.

(18) Harding, L. B.; Georgievskii, Y.; Klippenstein, S. J. *Journal of Physical Chemistry A* **2010**, *114*, 765.

(19) Zhang, X.; Friderichsen, A. V.; Nandi, S.; Ellison, G. B.; David, D. E.; McKinnon, J. T.; Lindeman, T. G.; Dayton, D. C.; Nimlos, M. R. *Rev. Sci. Inst.* **2003**, *74*, 3077.

(20) Vasiliou, A.; Nimlos, M. R.; Daily, J. W.; Ellison, G. B. *Journal of Physical Chemistry A* **2009**, *113*, 8540. See Figs. 3 (PIMS measurements) and 4 (matrix IR spectroscopy).

(21) Jochnowitz, E. B.; Zhang, X.; Nimlos, M. R.; Flowers, B. A.; Stanton, J. F.; Ellison, G. B. *Journal of Physical Chemistry A* **2010**, *114*, 1498.

(22) Heimann, P. A.; Koike, M.; Hsu, C. W.; Blank, D.; Yang, X. M.; Suits, A. G.; Lee, Y. T.; Evans, M.; Ng, C. Y.; Flaim, C.; Padmore, H. A. *Rev. Sci. Inst.* **1997**, *68*, 1945.

(23) Nicolas, C.; Shu, J. N.; Peterka, D. S.; Hochlaf, M.; Poisson, L.; Leone, S. R.; Ahmed, M. *Journal of the American Chemical Society* **2006**, *128*, 220.

(24) Daily, J. W.; Guan, Q.; Vasiliou, A.; Nimlos, M. R.; Ellison, G. B. *International Journal of Chemical Kinetics* **2011**, to be submitted.

(25) In studies at LBNL's Advanced Light Source, the threshold for observation of the m/z 43 peak at 1150 K was found to be as low as 10.1 eV. Consequently, given both experimental estimates of the room temperature threshold, and the bond energy $[CH_3CO\text{-}H]^+$ bond energy that we have calculated to be about 0.6 - 0.7 eV (which implies a 0 K threshold for $CH_3CHO \rightarrow CH_3CO^+ + H$ of about 10.8 - 10.9 eV), this suggests a substantial amount of vibrational excitation (of order 0.7 eV) in the 1150 K acetaldehyde. This seems to be very large, and is, in fact, inconsistent with preliminary studies of heated acetaldehyde vibrational states via chirped-pulse mm microwave spectroscopy [Kirill Kuyanov-Prozument and R. W. Field, unpublished results, 2011]. An alternative

explanation, which cannot be excluded at this point, is that the m/z = 43 signal comes from dissciative ionization of vinyl alcohol (CH_2=CH-OH), because *IE*(CH_2CHOH) ≤ 9.33 ± 0.05 eV. There might be a relatively low energy dissociative ionization channel leading to protonated ketene: $CH_2CHOH^+ \rightarrow CH_2=C=OH^+ + H$.

(26) Vasiliou, A.; Piech, K.; Zhang, X.; Reed, B.; Nimlos, M. R.; Ahmed, M.; Golan, A.; Kostco, O.; Osborn, D. L.; Daily, J. W.; Stanton, J. F.; Ellison, G. B. *Journal of Chemical Physics* **2011**, *(in preparation)*.

(27) Important ionization energies: *IE*(CH_3CHO) = 10.2298 ± 0.0007 eV; *IE*(CH_2=CHOH) ≤ 9.33 ± 0.05 eV; *IE*(H_2O) = 12.61737 ± 0.00025 eV; *IE*(CH_3) = 9.8380 ± 0.0004 eV; *IE*(CH_4) = 12.618 ± 0.004 eV; *IE*(CH_3CH_3) = 11.56 ± 0.02 eV; *IE*(HCCH) = 11.4006 ± 0.0006 eV; *IE*(CH_2O) = 10.8850 ± 0.0002 eV; *IE*(CH_2CH_2) = 10.51268 ± 0.00003 eV; *IE*(CH_2CO) = 9.617 ± 0.003 eV

(28) The commercial samples of CD_3CHO and CD_3CDO are produced by equilibrating acetaldehyde with D_2O and base. The proton NMR spectrum of the CD_3CHO sample shows that 6% is CD_2HCHO arising from incomplete proton/deuteron exchange. This is evident in the 118.2 nm PIMS in Fig. 1. The black trace for CD_3CHO shows a small feature at m/z 45 which is assigned to CD_2HCO^+ produced by dissociative ionization of CD_2HCHO. Likewise, the final red trace for CD_3CDO diplays a weak band at m/z 47 which is CHD_3CDO^+. The extent of impurity in the CD3OD sample, 2 %, was determined by integrating the corresponding peaks in the room temperature mass spectrum.

(29) Vasiliou, A.; Piech, K. M.; Nimlos, M. R.; Daily, J. W.; Stanton, J. F.; Ellison, G. B. *J. Molecular Spectroscopy* **2011**, *(in preparation)*.

(30) Hawkins, M.; Andrews, L. *Journal of the American Chemical Society* **1983**, *105*, 2523.

(31) Rodler, M.; Blom, C. E.; Bauder, A. *Journal of the American Chemical Society* **1984**, *106*, 4029.

(32) Joo, D. L.; Merer, A. J.; Clouthier, D. J. *Journal of Molecular Spectroscopy* **1999**, *197*, 68.

(33) Ni, C. K.; Wade, E. A.; Ashikhmin, M. V.; Moore, C. B. *Journal of Molecular Spectroscopy* **1996**, *177*, 285.

(34) The feature at m/z = 20 also arises, in part from Ar^{++}, which is always observed at the ALS facility due to stray high-energy radiation.

(35) Roberts, J. D.; Caserio, M. C. *Basic Principles of Organic Chemistry*; W. A. Benjamin, Inc.: Menlo Park, Calif., 1977. See pp 739-740

(36) Shimanouchi, T. *Tables of Vibrational Frequencies. Consolidated Volume I*; NSRDS-NBS 39, 1972. Methane has four vibrational modes but only the degenerate CH stretch, f_2 ν_3, and the degenerate deformation, f_2 ν_4, are IR active. In the gas-phase ν_3 CH_4 is observed at 3019.9 cm^{-1} and ν_4 CH_4 is found at 1306.2 cm^{-1}. These values shift in an Ar matrix to ν_3 = 3032 cm^{-1} and ν_4 = 1305 cm^{-1}. The signal from ν_4 is very intense and easy to detect in an cryogenic matrix.

(37) Huang, Y. B.; Yang, Y. A.; He, G. X.; Gordon, R. J. *Journal of Chemical Physics* **1993**, *99*, 2752.

(38) Burnett, S. M.; Stevens, A. E.; Feigerle, C. S.; Lineberger, W. C. *Chemical Physics Letters* **1983**, *100*, 124.

(39) Ervin, K. M.; Ho, J.; Lineberger, W. C. *Journal of Chemical Physics* **1989**, *91*, 5974.

(40) Gilles, M. K.; Lineberger, W. C.; Ervin, K. M. *Journal of the American Chemical Society* **1993**, *115*, 1031.

(41) Gunion, R. F.; Koppel, H.; Leach, G. W.; Lineberger, W. C. *Journal of Chemical Physics* **1995**, *103*, 1250.

(42) Gunion, R. F.; Lineberger, W. C. *Journal of Physical Chemistry* **1996**, *100*, 4395.

(43) Chen, Y. Q.; Jonas, D. M.; Kinsey, J. L.; Field, R. W. *Journal of Chemical Physics* **1989**, *91*, 3976.

(44) Jacobson, M. P.; Field, R. W. *Journal of Physical Chemistry A* **2000**, *104*, 3073.

(45) Hayes, R. L.; Fattal, E.; Govind, N.; Carter, E. A. *Journal of the American Chemical Society* **2001**, *123*, 641.

(46) Schuchma, H.; Laidler, K. J. *Canadian Journal of Chemistry* **1970**, *48*, 2315.

(47) da Silva, G.; Bozzelli, J. W. *Journal of Physical Chemistry A* **2006**, *110*, 13058.

(48) See P. R. Westmoreland's comments at the end of Gupte *et al.*'s 2007 paper.

(49) Liu, X. P.; Gross, M. L.; Wenthold, P. G. *Journal of Physical Chemistry A* **2005**, *109*, 2183.

(50) Acetaldehyde could rearrange to the vinyl alcohol *via* the methylhydroxycarbene: $CH_3CHO \rightarrow [CH_3\text{-}C\text{-}OH] \rightarrow CH_2{=}CH\text{-}OH$. But this pathway would predict that the vinyl alcohol resulting from CH_3CDO would be $CH_3CDO \rightarrow [CH_3\text{-}C\text{-}OD] \rightarrow CH_2{=}CH\text{-}OD$. Fig. 2 shows that the vinyl alcohol resulting from CH_3CDO is $CH_2{=}CD\text{-}OH$. Likewise, when CD_3CHO rearranges, we observe $CD_2{=}CHOD$ and not $CD_2{=}CD\text{-}OH$.

Table 1

A summary of thermal cracking products from acetaldehyde as identified by PIMS and IR spectroscopy.

1. $CH_3CHO + \Delta \rightarrow CH_3$ (PIMS) $\oplus$ CO (IR, PIMS) $\oplus$ CH_2CO (IR, PIMS) $\oplus$ CH_2=CHOH (IR, PIMS) $\oplus$ HC≡CH (IR, PIMS)

2. $CH_3CDO + \Delta \rightarrow CH_3$, CH_2D, CD_2H, CD_3 (PIMS) $\oplus$ CO (IR, PIMS) $\oplus$ CH_2CO (IR, PIMS) $\oplus$ CH_2=CDOH (IR, PIMS) $\oplus$ HC≡CH, HOD (IR, PIMS) $\oplus$ DC≡CH (IR, PIMS)

3. $CD_3CHO + \Delta \rightarrow CD_3$, CD_2H, CH_2D, CH_3 (PIMS) $\oplus$ CO (IR, PIMS) $\oplus$ CD_2CO (IR, PIMS) $\oplus$ CD_2=CHOD (IR, PIMS) $\oplus$ DC≡CH, D_2O (IR, PIMS) $\oplus$ DC≡CD, HOD (IR, PIMS)

4. $CD_3CDO + \Delta \rightarrow CD_3$ (PIMS) + CO (IR, PIMS) $\oplus$ CD_2CO (IR, PIMS) $\oplus$ CD_2=CDOD (IR, PIMS) $\oplus$ DC≡CD, D_2O (IR, PIMS)

Figure Captions

Fig. 1 Photoionization mass spectra of the thermal cracking products of acetaldehyde are shown. The fixed-frequency PIMS uses the 9th harmonic of a YAG laser, 118.2 nm or 10.487 eV, for photoionization. Samples of acetaldehyde entrained in He buffer gas are subjected to pyrolysis by a 1 mm x 2 cm SiC tube heated to 1500 K. Typical samples have 0.3 % acetaldehyde mixed with 2 atm He and are delivered to the μtubular reaction *via* a General Valve pulsed at 10 Hz. The approximate pressure in the μtubular reactor is 150 Torr and the centerline temperature is within 100 – 200 K of the wall temperature. The transit time through the heated SiC tube is roughly 50 — 100 μsec. There are 4 different spectra in this figure. Bottom Trace (black): CH_3CHO; 2nd Trace (red): CH_3CDO, 3rd Trace (black): CD_3CHO, 4th Trace (red): CD_3CDO.

Fig. 2 Matrix infrared absorption spectra of the thermal cracking products of acetaldehyde are shown. Samples of acetaldehyde entrained in an Ar buffer gas are subjected to pyrolysis by a 1 mm x 2 cm SiC tube heated to 1700 K. Typical samples have 0.3 % acetaldehyde mixed with 1 atm Ar and are delivered to the μtubular reaction *via* a General Valve pulsed at 10 Hz. The approximate pressure in the μtubular reactor is 75 Torr and the centerline temperature is within 100 – 200 K of the wall temperature. The transit time through the heated SiC tube is roughly 50 — 100 μsec. There are 3 different spectra in this figure. Bottom Trace (green): Ar carrier gas heated to 1700 K, 2nd Trace (black): CH_3CHO/Ar, 3rd Trace (red): CH_3CDO/Ar.

Fig. 3 The PIMS resulting from cracking CD_3CHO at 1400 K when the synchrotron at the LBNL's Advanced Light Source is used to photoionize the pyrolysis products. The tunable VUV light source is set to 12.9 eV in order to ionize methane,

acetylene and water. Samples of acetaldehyde-d_3 entrained in Ar buffer gas are subjected to pyrolysis by a 1 mm x 2 cm SiC tube heated to 1400 K. Typical samples have 1 % acetaldehyde mixed with 1 atm Ar and are delivered to the μtubular reaction *via* a General Valve pulsed at 10 Hz. The approximate pressure in the μtubular reactor is 75 Torr and the centerline temperature is within 100 – 200 K of the wall temperature. The transit time through the heated SiC tube is roughly 50 — 100 μsec.

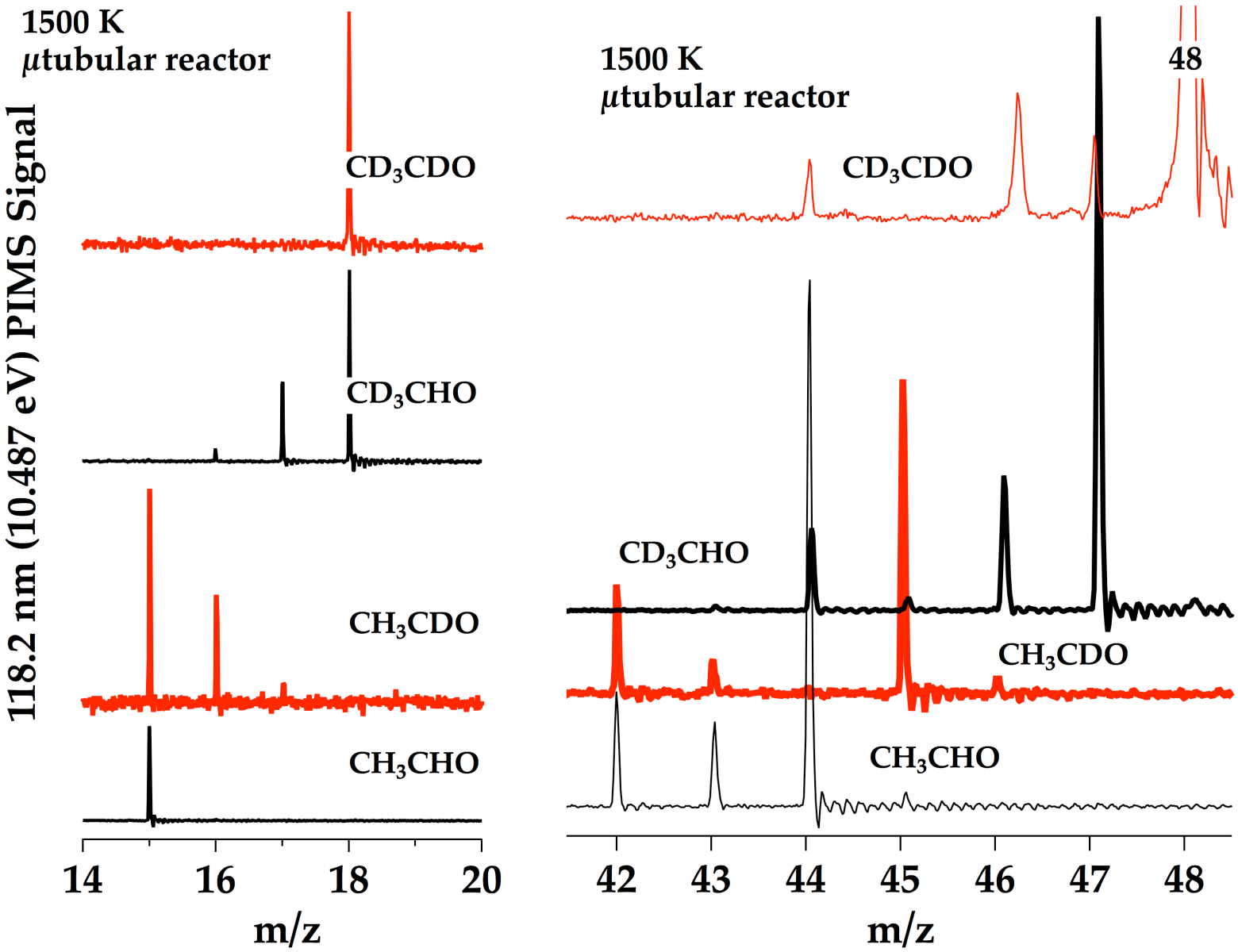
1500 K
μtubular reactor
118.2 nm (10.487 eV) PIMS Signal
CD3CDO
CD3CHO
CH3CDO
CH3CHO
14
16
18
20
m/z
1500 K
μtubular reactor
48
CD3CDO
CD3CHO
CH3CDO
CH3CHO
42
43
44
45
46
47
48
m/z

Fig. 1

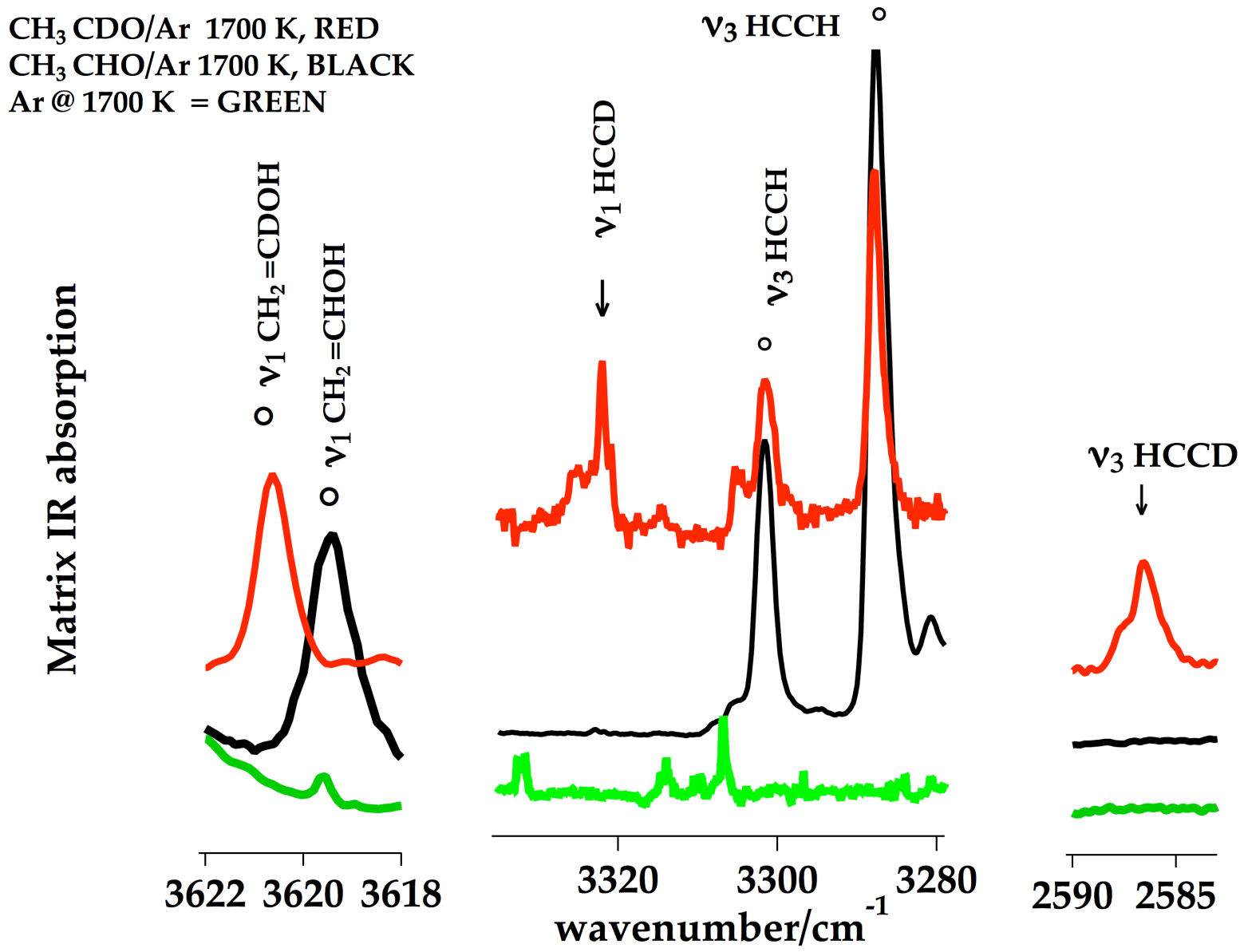
CH3 CDO/Ar 1700 K, RED
CH3 CHO/Ar 1700 K, BLACK
Ar @ 1700 K = GREEN
Matrix IR absorption
ν1 CH2=CDOH
ν1 CH2=CHOH
ν1 HCCD
ν3 HCCH
ν3 HCCH
ν3 HCCD
3622 3620 3618
3320 3300 3280
2590 2585
wavenumber/cm-1

Fig. 2

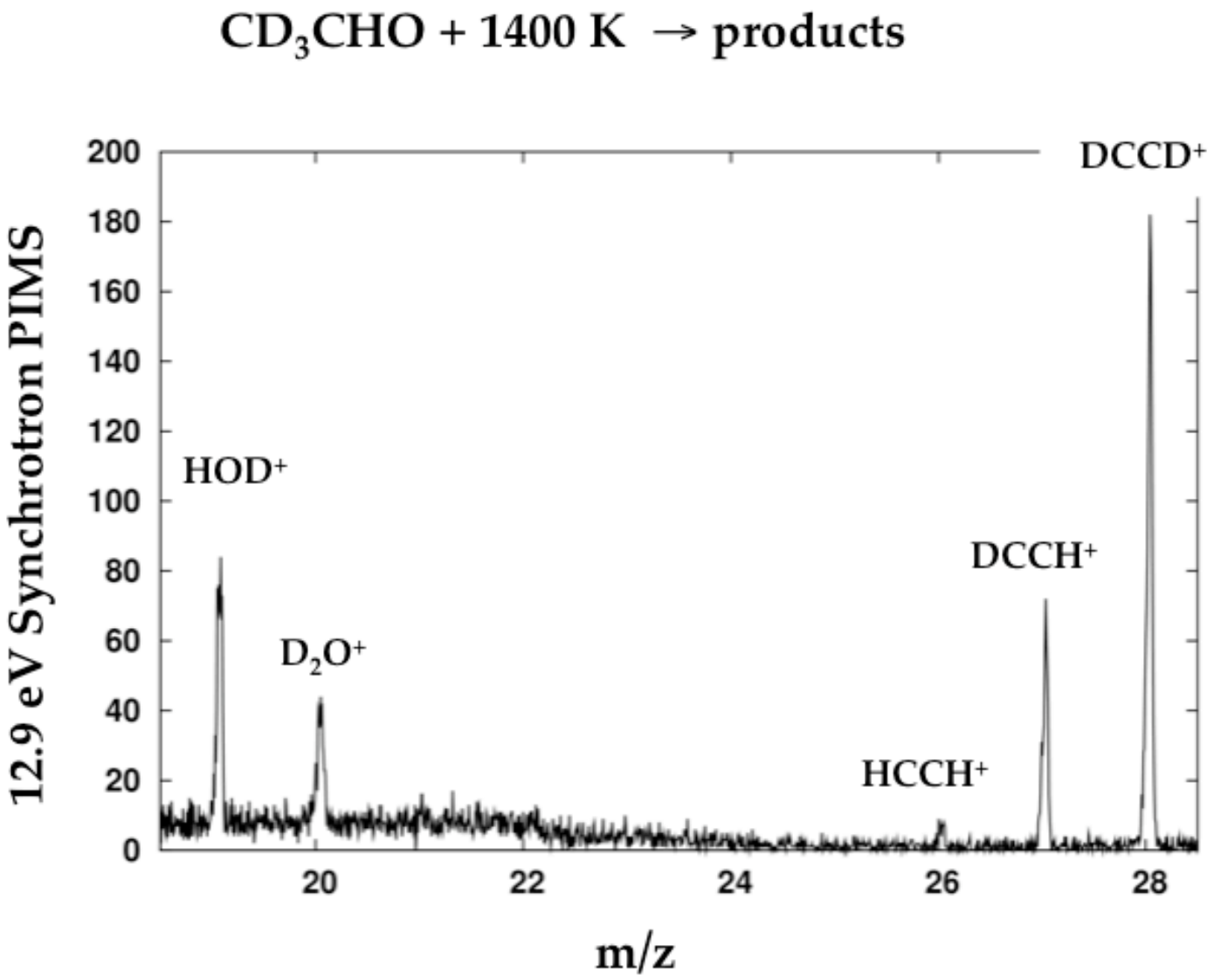
CD3CHO + 1400 K → products
12.9 eV Synchrotron PIMS
200
180
160
140
120
100
80
60
40
20
0
20
22
24
26
28
m/z
HOD+
D2O+
HCCH+
DCCH+
DCCD+

Fig. 3